We are IntechOpen, the world's leading publisher of Open Access books Built by scientists, for scientists

4,800
Open access books available

122,000
International authors and editors

135M
Downloads

Our authors are among the

154
Countries delivered to

TOP 1%
most cited scientists

12.2%
Contributors from top 500 universities

CLARIVATE ANALYTICS BOOK CITATION INDEX INDEXED

WEB OF SCIENCE™

Selection of our books indexed in the Book Citation Index in Web of Science™ Core Collection (BKCI)

Interested in publishing with us?
Contact book.department@intechopen.com

Numbers displayed above are based on latest data collected.
For more information visit www.intechopen.com

4

Ultrashort Pulses

Mikhail N. Polyanskiy and Marcus Babzien
Brookhaven National Laboratory
USA

1. Introduction

1.1 Niche for ultrashort-pulse CO_2 lasers

Ultrashort pulses usually are defined as those lasting less than a nanosecond. Low-energetic ultrashort pulses can be used, for instance, as a probe for studying the dynamics of ultrafast processes. Amplifying these pulses can deliver extremely high peak power, allowing applications such as laser particle acceleration, or γ-ray generation via Compton scattering on relativistic electrons. Existing laser systems can provide pulses as brief as hundreds of attoseconds (10^{-18} s) and as powerful as tens of petawatts (10^{15} W); more advanced ones are being constructed or are planned (Corkum & Krausz, 2007, Korzhimanov et al., 2011).

Virtually all modern ultrashort-pulse lasers are based on solid-state technology and usually operate at ~1 μm wavelength. Nevertheless, these applications relying not only on the ultrashort duration or the extreme power of the laser pulse, but also on its wavelength, leave a niche for laser systems utilizing different types of active medium. The 10-micron wavelength of the CO_2 laser particularly is beneficial for some usages.

To demonstrate the potential of ultrashort, mid-IR pulses, we consider their employment for laser ion acceleration, presently one of the main drivers for developing ultrashort-pulse CO_2 lasers (Palmer et al., 2011, Norreys, 2011). The motivation underlying the search for alternatives to conventional accelerators, wherein a system of electrodes and magnets creates the accelerating field, is the need to reduce the size and the cost of these devices. Acceleration in the electromagnetic field of a laser beam is a promising alternative for traditional acceleration schemes. In laser ion acceleration, an intense laser pulse focused on a target first ionizes it and then accelerates the charged particles from the resulting plasma. Usually this target is a metal foil, and a ~1 μm, multi-TW peak power, solid-state laser provides the ionizing/accelerating field. A very efficient acceleration regime called *Radiation Pressure Acceleration* (RPA) featuring a narrow energy-spectrum of the accelerated ions is reached when laser pulse interacts with plasma having a near-critical density (Esirkepov et al., 2004). The following formula defines critical plasma density, N_c (the density at which plasma becomes opaque):

$$N_c[\mathrm{cm}^{-3}] \approx 1.115 \times 10^{21} \left(\frac{n}{\lambda[\mu\mathrm{m}]} \right)^2 , \tag{1}$$

where n is the refractive index, and λ the laser wavelength. According to the Eq. (1), N_c is ~10^{21} cm^{-3} for the 1-μm lasers, and ~10^{19} cm^{-3} for the 10-μm lasers. These densities are much lower than that of solid materials. The critical density at 10 μm is comparable with the density of gases (~2.7×10^{19} cm^{-3} at 1 bar); thus, it readily is achievable for the CO_2 laser's wavelength when the gas jet is used as a target. On the other hand, realizing the critical-density jet for 1-μm solid-state lasers is challenging. Another advantage of the longer wavelength for ion acceleration in the RPA regime is the λ^2 scaling of the ponderomotive force, implying that a 100x lower intensity of the CO_2 laser field will suffice for reaching a given ion energy compared with a solid-state laser.

Yet another simple consideration favors CO_2 lasers for certain applications: A 10-μm laser pulse carries 10x more photons than a 1-μm pulse of the same energy. Photon density is important for applications such as γ-ray generation by Compton scattering on relativistic electrons (Yakimenko & Pogorelsky, 2006).

1.2 Challenge of high peak power

The minimum achievable duration of the pulse is defined by the bandwidth of the gain spectrum. In the simplest case of the absence of chirping (frequency variation with time), the spectrum of a pulse is the Fourier transform of its temporal profile. The pulse then is called transform-limited, and its duration, τ_p, is inversely proportional to its spectral width, $\Delta\nu_p$. The following expression is valid for a transform-limited Gaussian pulse (Paschotta, 2008):

$$\tau_p \approx \frac{0.44}{\Delta\nu_p}, \tag{2}$$

where τ_p and $\Delta\nu_p$ are defined as full-width at half-maximum (FWHM). The duration of a chirped pulse is longer than that of a transform-limited pulse of the same shape and spectral width. Fig. 1 shows the spectra of several femto- and pico-second transform-limited Gaussian pulses. Fig. 2 compares them with the gain spectrum of a typical CO_2 laser mixture, clearly revealing the challenge of generating and amplifying ultrashort pulses in a CO_2 laser.

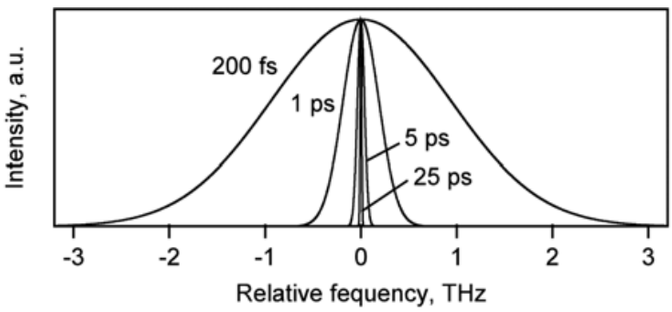

Fig. 1. Spectra of transform-limited Gaussian pulses. Durations are full-width at half-maximum (FWHM).

At low pressures (less than a few bars), the gain spectrum consists of individual rotational lines whose bandwidth (FWHM) is given by the following expression (Brimacombe & Reid, 1983):

$$\Delta\nu_{pressure}\left[\mathrm{GHz}\right] \approx P\left[\mathrm{bar}\right]\cdot\left(5.79\Psi_{CO2}+4.25\Psi_{N2}+3.55\Psi_{He}\right), \quad (3)$$

where P is the total gas pressure, and Ψ_x is the relative concentration of the component x. Eq. (3) yields $\Delta\nu_{pressure}\approx$3.8 GHz at 1 bar of a typical mixture [CO_2]:[N_2]:[He]=1:1:8. Although direct substituting this bandwidth in Eq. (2) gives $\tau_p\approx$120 ps, in reality the pulse's spectrum is narrower than the gain bandwidth, and, correspondingly, the pulse's duration is longer. The latter fact is comprehensible by realizing that amplification is the strongest in the center of the laser line, and thus, upon amplification, the ratio between the intensity at the central frequency and that at the wing of the gain-spectrum line increases, thus narrowing the pulse's spectrum. Consequently, the minimum achievable duration of the pulse for an atmospheric-pressure CO_2 laser is about 1 ns (Abrams & Wood, 1971). Pressure can be increased to broaden the gain bandwidth, and thus somewhat reduce the pulse's duration. However, the complete overlap of rotational lines separated by 55 GHz (P-) or 40 GHz (R-branches) that would allow using an entire rotational branch, does not occur below 20-25 bar; this is not feasible in discharge-pumped lasers having a ~10 bar practical pressure limit.

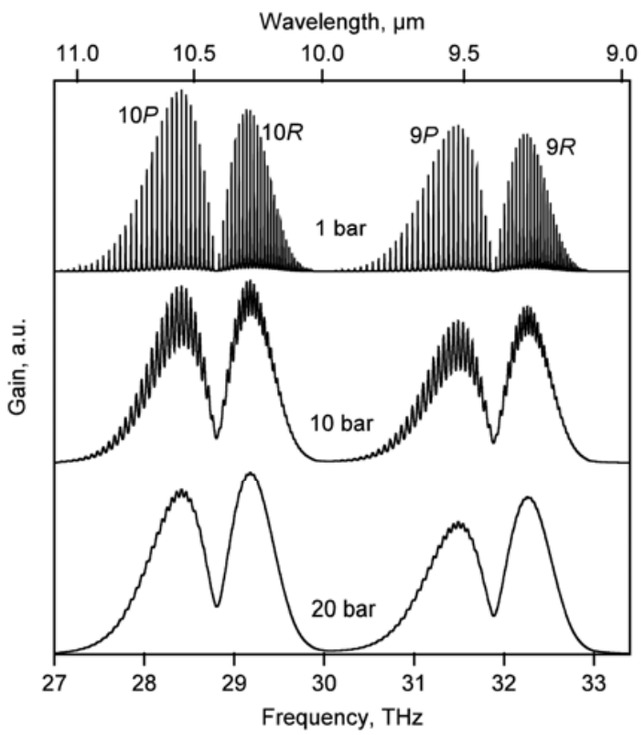

Fig. 2. Simulated normalized gain spectra at different gas pressures. 10P, 10R, 9P, and 9R: Rotational P- and R-branches of the two vibrational transitions supporting lasing at ~10 μm and ~9 μm respectively.

Another important consequence of the rotational structure of the CO_2 gain spectrum relates to the amplification of the ultrashort pulses. The spectrum of a few-picosecond-long pulse, according to Eq. (2), overlaps several rotational lines of the gain spectrum. Hence, upon amplification, the pulse's spectrum acquires the corresponding periodic structure. In the

time-domain (inverse Fourier-transform of the spectrum), this is equivalent to a pulse train with pulse-to-pulse distance equal to the inverse separation of the spectral lines (18 ps in the P-, and 25 ps in the R-branches). Fig. 3 demonstrates this effect for a 5-ps pulse amplified in a 10-bar active medium.

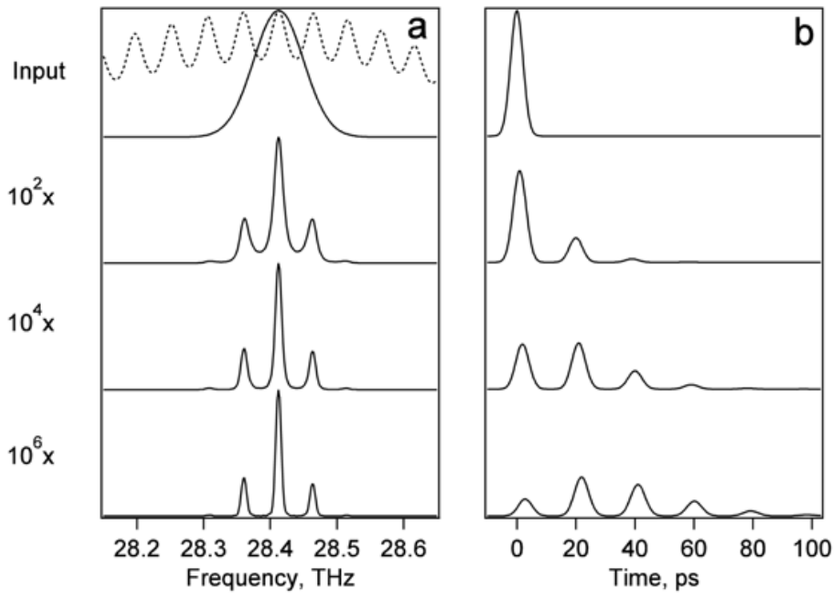

Fig. 3. Simulated dynamics of a 5-ps (FWHM) pulse spectrum (a), and its temporal structure normalized by the total energy in the train (b) amplified in a 10-bar CO_2 amplifier. Dashed line: normalized gain spectrum.

We discuss below different approaches to overcome these difficulties.

2. Generating the seed pulse

In all modern schemes for producing ultrahigh-power laser pulses there are at least two major stages: (1) Generation of a low-power, ultrashort seed pulse, and, (2) amplification of the pulse. In this section, we consider different methods of creating ultrashort 10-μm pulses. Section 3, following, discusses the amplification stage.

2.1 Mode-locking

Mode-locking is the primary technique of generating ultrashort pulses in solid-state systems. In this approach, cavity modes present in the spectrum of the laser field are synchronized (locked) by modulating the cavity's Q-factor at a frequency that is a multiple of the inverse of the resonator's round-trip time, either actively (e.g., with an intra-cavity acousto-optical modulator), or passively (e.g., with a saturable absorber). Without synchronization, each mode is independent and defines its own pulse; thus, the pulse's duration is only limited by the relatively narrow bandwidth of an individual mode. However, after mode-locking, the time structure of the laser field is defined by the entire spectrum comprising *all* active modes. For the periodic spectrum of longitudinal modes, this structure is a periodic train of pulses; the pulse's repetition rate is equal to the lock-in

frequency (i.e., a multiple of the inter-mode distance), and individual pulse's duration is inversely proportional to the total extent of the spectrum.

The minimum pulse duration achievable via mode-locking is related to the bandwidth, $\Delta\nu$, (FWHM) of the gain spectrum according the following expression (Siegman & Kuizenga, 1969):

$$\tau_p \approx 0.45 \cdot \left(\frac{g}{M}\right)^{1/4} \left(f \cdot \Delta\nu\right)^{-1/2}, \tag{4}$$

where $g \equiv 2aL$ is the saturated round-trip excess gain (a – excess gain per unit length, L – resonator length), M is the modulation, and $f=c/2L$ is its frequency. For a typical transversely excited atmospheric pressure (TEA) CO_2 laser (g=1; M=1; f=150 MHz; $\Delta\nu$=3.8 GHz) the duration is $\tau_p \approx 600$ ps. Wood et al. describe their technical realization of the mode-locked TEA CO_2 laser (Wood et al., 1970, Abrams & Wood, 1971). A 10-bar mode-locked system was reported by Houtman and Meyer (Houtman & Meyer, 1987). Application of mode-locking is limited in 10-micron systems by relatively long (hundreds of picoseconds) pulse duration achievable via this technique.

Passive self-mode-locking often occurs in TEA CO_2 lasers producing a comb pulse-structure unless special countermeasures are taken. This effect is believed to be due to gain saturation (Kovalev, 1996). When a smooth pulse is required, the laser must be forced to operate at a single cavity mode that usually is achieved by using a low-pressure intra-cavity CW discharge cell ("smoothing tube"). Such a laser, combining two gain sections in a single resonator; viz., main atmospheric-pressure and a low-pressure one for spectrum narrowing, is called *hybrid* laser. Fig. 4 is an example of a hybrid TEA CO_2 lasers' pulse profile with and without discharge in the smoothing tube. As Fig. 4a shows, self-mode-locking occurring when the smoothing tube not activated results in modulation at a frequency that is a multiple (here, double) of the inter-mode spacing. Activating the smoothing tube eliminates the modulation, Fig. 4b.

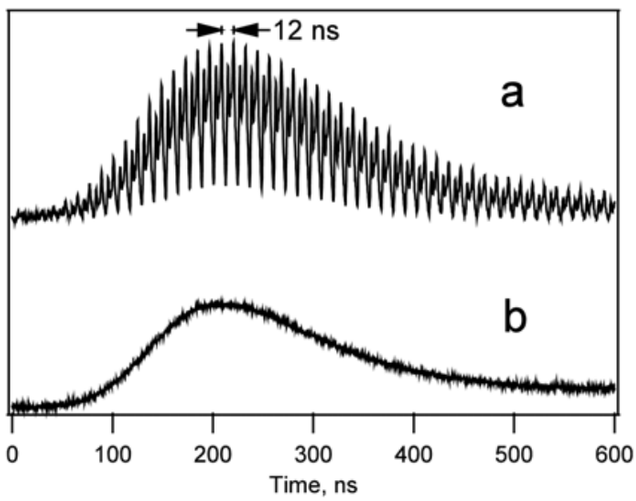

Fig. 4. Temporal structure of the output of a hybrid TEA CO_2 laser with smoothing tube discharge OFF (a), and ON (b). Resonator round-trip time is 12 ns; self-mode-locking occurs at the doubled round-trip frequency.

2.2 Plasma shutter and optical free-induction decay

Highly intense laser pulses focused in gas media can initiate avalanche ionization (laser breakdown). If gas density is high enough, overcritical plasma forms, blocking the trailing part of the laser pulse, partially absorbing and partially reflecting it. This effect itself, usually termed *plasma shutter*, can be used to cut the tail of the pulse thus reducing its overall duration. However, it is not sufficient for producing an ultrashort pulse because the front part of the initial pulse passes the plasma shutter unchanged. The possibility of generating a pulse as short as a few optical cycles lies in the fact that the fast switching-out of the laser field by plasma entails a very rapid variation in the field spectra. Essentially, we can approximate the spectrum of the transmitted pulse by the Fourier-transform of a step function. Frequencies different from those present in the original pulse briefly appear in the spectrum. If we now filter-out the frequency of the initial pulse from the resulting spectrum, we end up with a very short pulse (Yablonovich, 1973, 1974a, 1974b). Free-induction decay technique is relatively simple to realize and can allow achieving ~20 ps pulse duration at the expense of large losses and strong alteration of the spectrum.

2.3 Pulse-slicing techniques

Another possibility for producing a low-energy ultrashort pulse is to slice a small fraction out of a longer one (for instance, a hundred-nanosecond output of a hybrid TEA CO_2 laser similar to that in Fig. 4b) using a fast optical switch. Here, the switching speed limits the duration of the resulting pulse. Two techniques often employed for this purpose are a semiconductor optical switch (Alcock & Corkum, 1979), or a Kerr cell (Filip et al., 2002). Both rely on an ultrashort pulse of another laser (usually a solid-state one) to trigger the switch by inducing a short-living "plasma mirror" in the case of a semiconductor switch, or birefringence in that of the Kerr cell. Fig. 5 illustrates the principles of these two techniques.

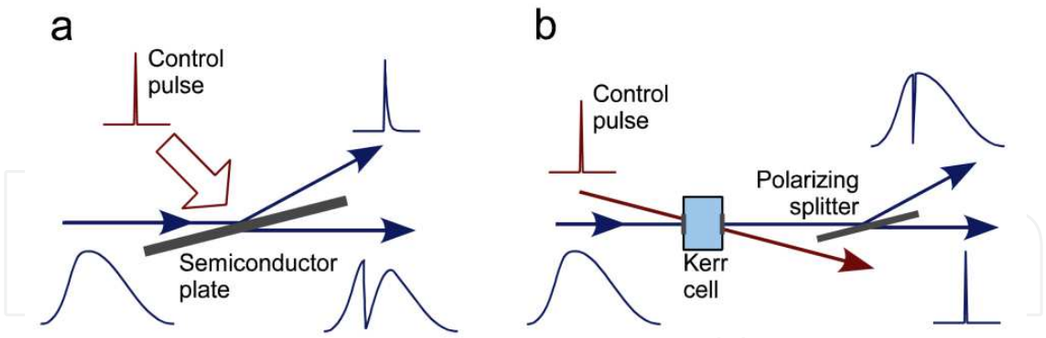

Fig. 5. Simplified schematics of the techniques for pulse slicing by (a) the semiconductor switch, and, (b) the Kerr cell.

A powerful laser pulse irradiating the surface of a semiconductor partially ionizes it creating a "plasma" of free charge carriers. If the plasma's density exceeds the critical one (N_c), the semiconductor surface turns into a mirror, reflecting the entering laser beam. At below-critical densities, the beam is attenuated mostly by free-carrier absorption. The duration of the reflection is determined mainly by that of the control pulse, and the speed of free carrier diffusion (typically hundreds of picoseconds). Absorption generally lasts longer (hundreds of nanoseconds), and its persistence is defined by the free carrier's recombination time. The

inverse-quadratic relationship between N_c and the laser's wavelength (Eq. (1)) allows our realization of a scheme wherein a relatively low-energy pulse from a solid-state laser controls a high-power CO_2-laser pulse. Combining two semiconductor switches, the first of which operates in a reflection- and the second in the transmission- configuration (Fig. 6) enables us to slice a CO_2 pulse on both edges, thus producing one whose duration is limited only by the rise-time of the control pulse.

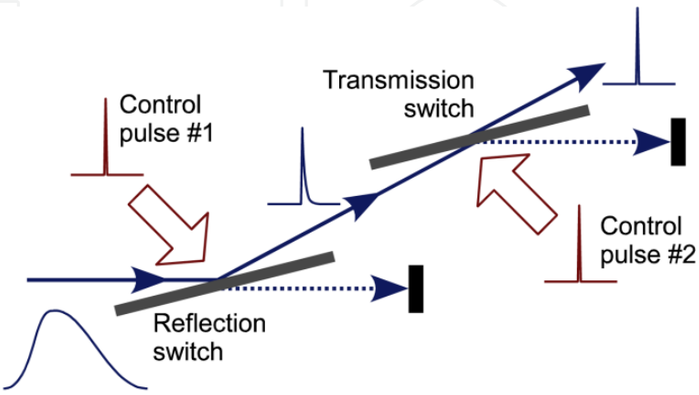

Fig. 6. Combination of reflection- and transmission- semiconductor switches to generate an ultrashort pulse.

Reportedly, Rolland & Corkum, (1986) achieved a 130-fs pulse via this technique. Germanium is the commonest material used in semiconductor switches; silicon and cadmium telluride also proved usable in this application.

The laser-stimulated birefringence employed in the Kerr-cell technique has the advantage of low inertness, so supporting the production of an ultrashort pulse in a single step. Its minimum achievable duration is limited by that of the control pulse, and the relaxation speed of the induced birefringence. The Kerr cell depicted in Fig. 5b rotates the polarization of the CO_2 laser-beam while it is being irradiated by the control pulse. A polarization filter on the cell output separates the part of the pulse with rotated polarization from the main pulse. Liquid carbon disulphide (CS_2) featuring ~2 ps relaxation time usually serves as the active medium in the optical Kerr cell for slicing the CO_2 laser pulses. For optimum switching efficiency, the phase angle between the control- and the CO_2 laser- pulses must be equal to $\pi/4$.

Currently, pulse-slicing is the main method of producing low-energy ultrashort (few-picosecond) 10-micron seed pulses.

2.4 All-solid-state systems

Solid-state ultrafast oscillators producing several-cycle and longer optical pulses in the near-infrared spectral region are a well-established technology. Using frequency conversion via *optical parametric amplification* (OPA) one can generate an ultrashort mid-IR pulse. One of the earliest theoretical treatments of parametric amplification was by Armstrong, Bloembergen, Ducuing, and Pershan (Armstrong et al., 1962). Using a resonant cavity to enhance output, Giordmaine and Miller demonstrated the principle (Giordmaine and Miller, 1965). Okorogu et al. demonstrated efficient, single-stage difference frequency downconversion from near-

to mid-IR (Okorogu et al., 1998). The combination of compact size, various free-space or fiber-based configurations, and efficient pump sources provide an advantageous starting point for CO_2 laser seed sources. One method used for frequency conversion is covered below with attention toward stable and reliable operation as a sub-component of a larger CO_2 laser system.

Titanium-doped sapphire is now the dominant laser system in many industrial and research fields such as physical chemistry, materials science and processing, and strong-field physics. Therefore, a large commercial infrastructure exists for producing reliable amplifiers delivering high energy pulses suitable for nonlinear conversion. Diode-pumped Neodymium lasers which are frequency-doubled for pumping the broadband Ti:Al_2O_3 gain medium are turn-key and have lifetimes on the order of 10 000 hours. Many amplifier systems are available producing pulse energies above 5 mJ near 1 kHz repetition rates. In such a configuration, the pump pulses have energy stability better than 1% because the energy is removed on a time scale comparable to the upper-state lifetime, and a quasi-steady-state exists between pumping and energy extraction.

After amplification to high energy, the use of OPA provides a path for the generation of significant seed energies at 10 μm with the full bandwidth and tunability to cover the entire gain spectrum of CO_2. One such commercial approach is shown in Fig. 7.

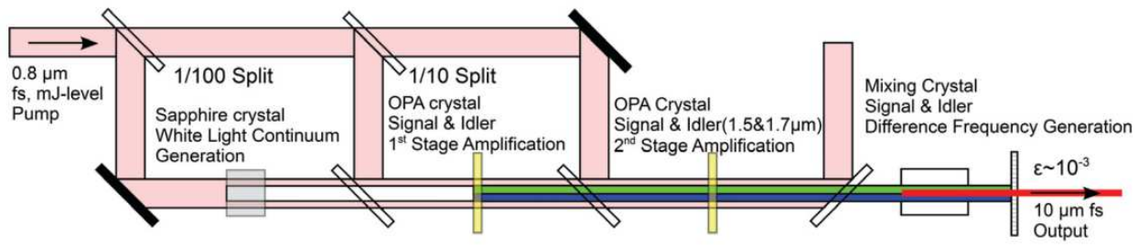

Fig. 7. Commercially-available frequency conversion system from 0.8 to 10 microns

In this configuration, the pulses from the Ti:Al_2O_3 amplifier are used in three separate nonlinear processes. The first is white light continuum generation in sapphire. This process creates an ultra-broadband spectrum spanning the entire visible and near-IR region while preserving the phase and temporal structure of the original pulses. This broadband radiation makes an ideal seed source for the following sections as it allows free tuning to the desired wavelengths. Because the next section uses three-wave mixing, this seed power also eliminates instabilities that would be encountered from quantum fluctuations in a pure parametric generator.

The next two stages rely on standard nonlinear crystals and act as simple parametric amplifiers that are angle-tuned to achieve gain at the desired signal and idler wavelengths. For conversion from 0.8 to 10 micron, these are approximately 1.5 and 1.7 micron, respectively. By utilizing two stages, the gain of each section can be optimized while preserving bandwidth that would be limited by a longer single crystal. The second parametric amplification stage therefore utilizes most of the pulse energy delivered from the Ti:Al_2O_3 amplifier.

In the final section, the signal and idler from the previous stages generate a difference frequency pulse in another nonlinear material that has transparency in the mid-IR region.

These cascaded nonlinear processes allow stable, repeatable conversion of the ultrafast pump pulses from the near- to the mid-IR region, while providing broad bandwidth, wavelength tunability, and ultrashort duration. The theoretical maximum energy conversion efficiency from 0.8 to 10 micron via this cascaded three-photon mixing is near 3.5%, however when real beams which are non-uniform in time and space are considered, as well as losses on the large number of optical elements required, the realized efficiency is approximately an order of magnitude lower. Pulsewidths under 500 fs are easily achievable, as well as bandwidth covering any single branch of the CO_2 gain spectrum.

All-solid-state systems provide good control of pulse synchronization and shape, but are much more elaborate than the other techniques used for ultrashort mid-IR pulse generation.

3. Amplification

3.1 "Smoothing" the gain spectrum

A major problem in seamlessly amplifying picosecond pulses is the discrete rotational-line structure of the gain spectrum, causing modulation of the pulse spectrum and pulse splitting. The gain spectrum's modulation can be smeared either by broadening individual rotational lines, thus assuring their better overlap, or by increasing their density. In the first case, we can use pressure- (collision-) and/or field- (power-) broadening effects. Several approaches increase line density: (1) Using an R-branch of a laser transition having a 1.4 times denser line structure than a conventional P-branch; (2) isotopic enrichment of the CO_2 molecules, wherein the superposition of the slightly shifted spectra of different isotopic species (*isotopologues*) generates a denser effective spectrum; and, (3) combining the *sequence* bands of laser transition with regular ones. We briefly overview these approaches next.

Pressure broadening. As discussed in the Section 1.2, increasing the pressure lowers modulation in the gain spectrum. Complete suppression occurs when collisionally broadened bandwidths of the rotational lines become about twice the interline distance. However, the 20-25 bar pressure required for this, according to the Eq. (3), is impractical due to difficulties in arranging the uniform electric-discharge pumping the large volume of active gas required for building a high-power CO_2 laser amplifier. Replacing discharge- with optical- pumping may afford using a pure-CO_2 active medium and increased working pressure, thus considerably extending the pressure broadening effect. Rapid progress in the solid-state laser technology might well lead to the availability of a reliable source for optical excitation of CO_2 active medium in the near future. Gordienko & Platonenko, (2010) consider that here the ErCr:YSGG (2.79 μm) laser is a promising candidate.

Field broadening. We can approximate the magnitude of line broadening (FWHM) appearing in the intense laser field due to the Autler-Townes (or dynamic Stark) effect (Autler & Townes, 1955) by the doubled Rabi frequency Ω: $\Delta\nu_{field} = 2\Omega = 2\frac{d \cdot E}{h}$, where d is the transition dipole momentum, E is the laser field, and h is Plank's constant. Substituting the laser field with its expression through the intensity, I, and using the numerical values of the involved constants, we get the following equation:

$$\Delta\nu_{field}[\mathrm{GHz}] \approx 0.02764\, d[\mathrm{D}] \sqrt{I[\mathrm{W/cm^2}]} \tag{5}$$

With Eq. (5), and the known value of the laser's transition dipole momentum d=0.0275 D (the value for the 10P(20) line from HITRAN database (Rothman et al., 2009)), we find that field broadening is sufficient to completely suppress modulation at a laser intensity 15-20 GW/cm^2; this is reachable in the modern high-power picosecond CO_2 laser systems. Capitalizing on this approach supported the attainment of 15 TW peak power in the CO_2 laser system of Neptune Laboratory of the University of California, Loss Angeles (Section 6.2).

R-branch. The R-branches of the CO_2 laser transitions have a rotational structure 1.4 times denser than the more often used P-branches (Witteman, 1987); thus, they offer better overlap between collisionally broadened lines, and, hence, yield a smoother gain spectrum (Fig. 2). Interestingly, under high-pressure conditions, such as 10 bar or higher, the overlap between rotational lines increases the peak intensity of the R-branch compared to that of the P-branch that otherwise prevails in conventional low-pressure lasers.

Isotopic CO_2. By partially substituting the ^{16}O atoms in CO_2 gas with another stable ^{18}O isotope, we obtain almost perfectly smooth combined spectrum after superimposing the spectra of three CO_2 isotopologues (molecules with different isotopic composition): ^{16}O-^{12}C-^{16}O, ^{16}O-^{12}C-^{18}O, and ^{18}O-^{12}C-^{18}O (Fig. 8). They often are denoted as 626, 628, and 828 wherein 2, 6, and 8, respectively, represent ^{12}C, ^{16}O and ^{18}O.

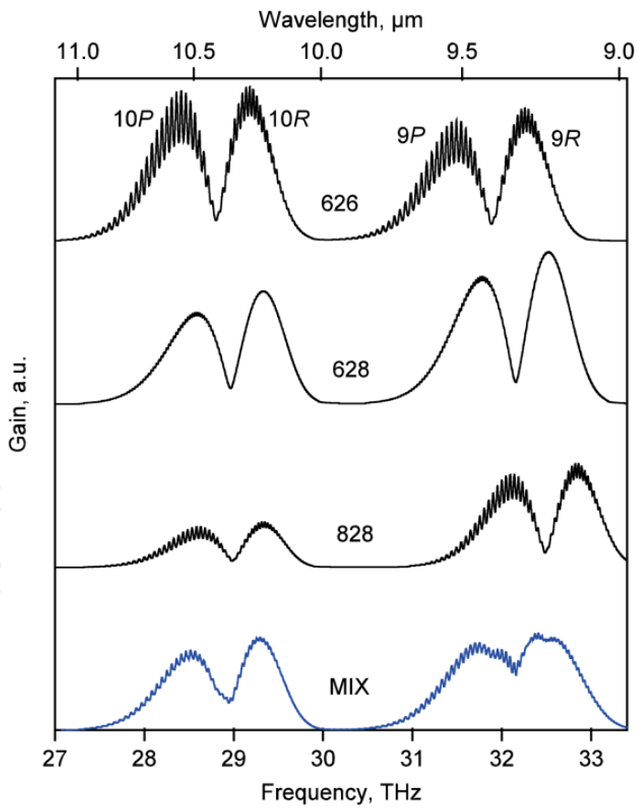

Fig. 8. Simulated gain spectra of three CO_2 isotopologues with different combinations of oxygen-16 and oxygen-18 atoms (no enrichment in carbon isotopes), and the effective spectrum of their mixture in the proportion [626]:[628]:[828]=0.16:0.48:0.36 (statistical equilibrium in the case of [^{16}O]:[^{18}O]=0.4:0.6). Total gas pressure is 10 bar.

For a given proportion [^{16}O]:[^{18}O], independent of the initial distribution of ^{16}O and ^{18}O between the CO_2 molecules, statistical equilibration via intermolecular isotope-exchange leads to [626]:[628]:[828]= [^{16}O]^2:2[^{16}O] [^{18}O]:[^{18}O]^2. We note that due to the broken symmetry of the 628 molecule, it has twice as many rotational lines in each rotational branch compared to more symmetric 626- and 828- isotopologues. The combination of three CO_2 isotopologues, as depicted in Fig. 8, results in a smooth spectrum already apparent at 10 bar. The gain of the isotopic mixture in the 10-micron branches at this pressure is 1.4 times lower than that of the regular gas, mainly reflecting the relatively low gain of the 828 CO_2 isotopologue. Thus, a longer path through an active medium or a higher CO_2 concentration is needed to maintain the same net amplification. The isotope-based approach is practically implemented in the CO_2 laser of Accelerator Test Facility at Brookhaven National Laboratory (Section 6.1).

Sequence bands. Transitions between high-lying vibrational overtones of the CO_2 molecule can contribute considerably to the high-pressure amplifier gain. In this case, the rotational spectra of the regular- and sequence- bands overlap, so providing a denser effective spectrum. Exploiting the sequence band for smoothing the gain spectrum seems especially promising for the 10R branch wherein the rotational lines belonging to the sequence band 00^02-$[10^01,02^01]_I$ fall very close to the centers of the gaps between the lines of the regular band 00^01-$[10^00,02^00]_I$. Simple estimation of the ratio of gains of the sequence- and the regular- band, assuming the Boltzmann energy distribution within a vibrational mode (Reid & Siemsen, 1976):

$$G_{seq} / G_{reg} = 2\exp(-h\nu_3 / kT_3), \tag{6}$$

where T_3 and ν_3 are the vibrational temperature and frequency of the asymmetric stretch-mode of the CO_2 molecule, and h and k respectively are the Plank's and Boltzmann's constants, show that sequence band's gain reaches 50% of the regular band's gain at T_3=2500 K, viz., comparable to the conditions of high-pressure CO_2 amplifiers.

3.2 Effects in optical materials

To assure highly intense laser fields, special attention must be given to properly selecting and utilizing the optical elements, and to accounting for their influence on the laser field. This especially is challenging in the 10-μm spectral region because of the dearth of optical materials compared to the visible or near-IR diapasons, and lack of data on the materials' behavior under ultrashort mid-IR pulses. Below, we summarize the properties of optical materials most important for using in the high-peak-power 10-μm laser field. Table 1 gives numerical data on the refractive indices and dispersion of some popular IR materials used in CO_2 lasers.

Chromatic dispersion plays an important role due to the hundreds of GHz-wide spectrum of (sub-) picosecond 10-μm pulses that may entail considerable pulse stretching. For example, a pulse of 1 ps (FWHM) spreads to 1.27 ps after a single pass through a 10-cm NaCl window. Accordingly, the amount and thickness of optical elements should be minimized, and/or a grating compensator added for recompressing the pulse.

Nonlinear index, B-integral. A high-power laser pulse propagating through a medium changes its refractive index n (the *Kerr effect*):

$$n = n_0 + n_2 I \ , \tag{7}$$

where n_0 is the linear (low-intensity) refractive index, n_2 the nonlinear index, and I the optical intensity. Variation of refractive index across the beam's cross-section degrades its quality. For instance, lensing (*Kerr lensing*) occurs when phase-shift in the center of the beam is considerably larger than on its edge. The additional phase-retardation introduced to the beam after propagating through an optical element due to the nonlinear index (*B-integral*) is the accepted parameter for quantifying this effect (Paschotta):

$$B = \frac{2\pi}{\lambda} \int n_2 I(z) dz \ , \tag{8}$$

where λ is the wavelength, $I(z)$ the optical intensity along the beam's axis, and, z the position in the beam's direction. Usually, a noticeable self-focusing occurs if the B-integral exceeds 3-5. Strong wave-front distortion and eventually catastrophic filamentation may occur at larger values of the B-integral. An estimate of the B-integral using the n_2 index from the Table 1 yields B = 13.4 for a 1 ps (FWHM), 500 mJ/cm² pulse passing through a 10 cm of NaCl. Expectedly, the effect will be much stronger for other materials, implying that special care must be taken in selecting materials and controlling the fluence through the optical elements. The Kerr effect also is responsible for self-chirping due to temporal variation of the phase shift defined by the pulse's temporal structure (see Section 4.1).

	n_0 @ 10.6 μm [a]	$dn_0/d\nu$ @10.6 μm (10^{-3} THz^{-1}) [a]	n_2 (10^{-16} cm²/W) [b]
KCl	1.45	1.51	5.7 @ 1.06 μm
NaCl	1.49	2.64	4.4 @ 1.06 μm
ZnSe	2.40	2.44	290 @ 1.06 μm
CdTe	2.67	1.04	-3000 @ 1.06 μm
Si	3.42	0.0914	1000 @ 2.2 μm[c]
Ge	4.00	0.293	2800 @ 10.6 μm

Table 1. Linear refractive index n_0, chromatic dispersion $dn_0/d\nu$, and nonlinear index n_2 of some IR materials. (a) RefractiveIndex.INFO; (b) Sheik-Bahae et al., 1991; (c) Bristow et al., 2007.

Optical breakdown threshold. We know far less about the ultrashort-pulse breakdown thresholds for mid-IR wavelengths and the materials used at these wavelengths than we do for visible light and near-IR. Reportedly, the values are ~0.5 J/cm² for NaCl, and 1-2 J/cm² for gold-coated stainless-steel mirrors for 2-ps, 10-μm pulse (Corkum, 1983). Variations in the breakdown threshold with pulse duration are best studied for fused silica at a wavelength of ~800 nm (Du et al., 1994, Stuart et al., 1996, Tien et al., 1999). Jia et al. (2006) also explored the wavelength dependence of the damage threshold over 250-2000 nm for 150 fs pulses; they concluded that there was a relatively small variation in the threshold at wavelengths above 800 nm. At pulses <10 ps, the damage threshold decreases slow with declining duration of the pulse, rather than displaying the $\tau_p^{1/2}$ dependence valid for longer pulses; this difference is explained by the gradual transition from a thermally dominated damage regime to one dominated by collisional- and multi-photon- ionization and plasma

formation. Assuming a similar behavior in mid-IR, we conclude there is relatively small variation of the breakdown threshold fluence as a function of pulse duration for pulses of a few picoseconds or shorter; thus, as a guideline in system design, in most cases we can adopt 0.5 J/cm^2 for transparent optics, and 1 J/cm^2 for mirrors.

3.3 Chirped-pulse amplification

We can minimize the high-power effects in optical materials on the pulse by employing the method of chirped-pulse amplification (CPA), the principle of which is illustrated in Fig. 9.

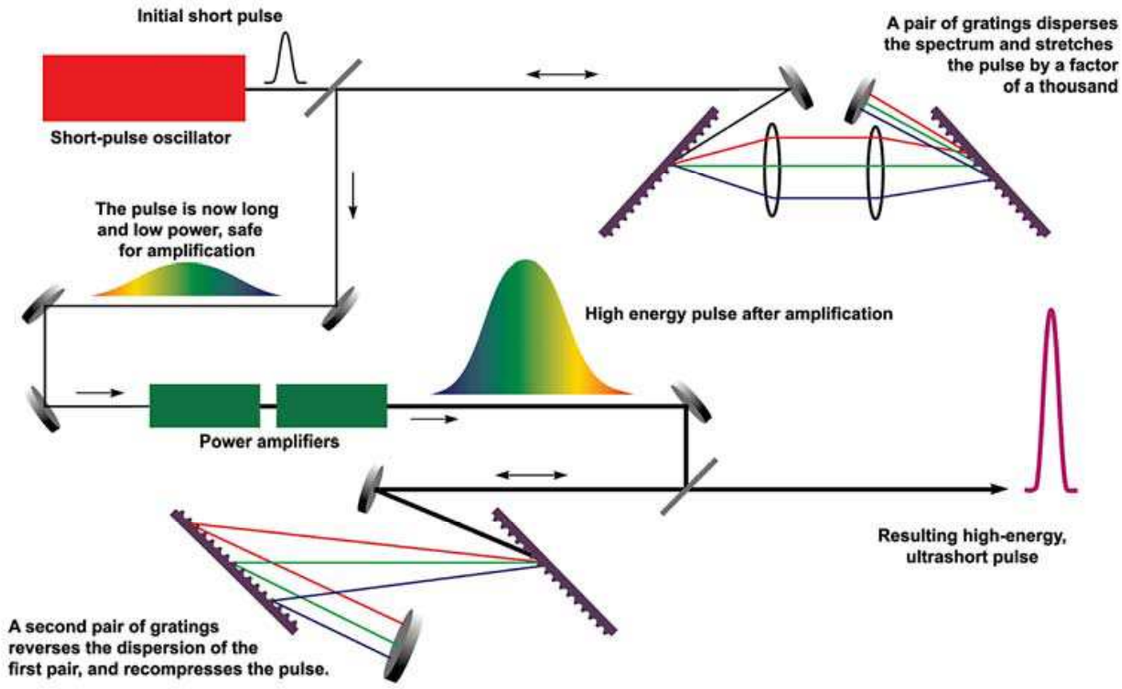

Fig. 9. Chirped-pulse amplification schematic (Perry et al., 1995). Reproduced with permission, courtesy of the Lawrence Livermore National Laboratory.

Before being amplified, an ultrashort pulse is *chirped*: A wavelength-dependent delay is introduced in the pulse using a *stretcher* consisting of a couple of gratings and lenses, as shown in the Fig. 9. Because ultrashort pulses have broad spectral bandwidth, inversely proportional to their duration (Eq. (2)), it is relatively straightforward to stretch them by a few orders-of-magnitude. The chirped pulse carries virtually the same energy as the original one, but its peak power is reduced in inverse proportion to the stretching factor. The chirped pulse can be amplified to energies much higher than that achievable by directly amplifying ultrashort pulses wherein high-power effects in optical materials and active medium appear earlier. After amplification, the pulse is re-compressed in another two-grating device (the *compressor*).

The invention of CPA for reducing light intensity during ultrashort pulse amplification was a dramatic breakthrough in solid-state laser technology. Although implementing the CPA technique in a (sub-)picosecond CO_2 laser remains to be done (the corresponding project is

planned at the Accelerator Test Facility of the Brookhaven National Laboratory), it is reasonable to expect that the outcome will comparably be valuable.

3.4 Energy extraction efficiency

Optimal use of the energy stored in the active medium is a key characteristic of a mature laser design. The difficulty in efficiently extracting excitation energy from gaseous active media via an ultrashort pulse arises from the fact that the pulse's duration is either shorter than, or comparable to the characteristic times of the involved excitation- and relaxation-processes. Below, we briefly consider these processes and their influence on the efficiency of extracting energy.

Excitation and vibrational relaxation. In a typical CO_2 laser, an electric discharge is used to create population inversion. Fast electrons accelerated by electric field collide with CO_2 and N_2 molecules, so exciting their upper vibrational states. Nitrogen serves as reservoir for storing the excitation energy which is then transferred to CO_2 via vibrational relaxation. The typical duration of discharge in a pulsed CO_2 laser is about a microsecond, and vibrational relaxation times range from 1-10 ns·bar. This implies that a (sub-)picosecond laser pulse only extracts energy already available at the upper vibrational laser-level, with negligible energy deposition from the discharge or from redistribution from other vibrational levels during pulse propagation. To maximize extraction, wherever possible a regenerative amplification scheme is used, wherein the pulse passes the amplifier medium many times allowing repopulation of the upper vibrational level of the laser transition between the passes. However, realizing this scheme practically is problematic for high-energy pulses when beam must be wide to increase the active volume and avoid damaging optical elements. Thus, two-stage amplification usually is adopted (see Section 6); a regenerative amplifier providing amplification up to millijoules level is followed by a final high-energy amplifier arranged either in a single-pass configuration, or several passes are only partially overlapped. Slow pumping and vibrational relaxation limit energy extraction in the final amplification stage. A possible solution is replacing pumping by electric discharge, with optical pumping by a short laser pulse that quickly and directly excites the upper laser level, and eliminates the need for redistributing vibrational energy.

Rotational relaxation. Rotational relaxation processes limit the fraction of energy extractable from the upper vibrational laser level in a single pass through the active medium. The laser pulse interacts only with a limited number of rotational transitions that is defined by the overlap between the pulse's spectrum and the amplification band. At high pressure, when collisionally broadened rotational lines overlap, or for a very short pulse, when pulse's spectrum covers several rotational lines, energy is extracted from several rotational sub-levels. Otherwise, energy is extracted only from a single sub-level containing about $1/15^{th}$ of the entire energy stored in that vibrational level. Three scenarios support the complete emptying of the vibrational level: (1) The pulse is long enough to provide time for repopulation of the active rotational levels. Typical rotational relaxation times are ~100 ps·bar; about 15 collisions are required effectively to empty all rotational sub-levels through a single active rotational transition. Thus, the minimum required pulse duration is ~1.5 ns·bar (e.g., 150 ps at 10 bar). (2) Pressure broadening allows all rotational transitions to interact with the laser field. Using Eq. (3) we find that ~100 bar is needed to broaden the

rotational lines to the ~0.5 THz necessary for this regime. (3) The spectrum of the pulse covers the entire rotational branch, as happens when the pulse duration is ≤1 ps (Eq. (2)). The last regime is preferable if the aim is to keep pulse's span as brief as possible.

4. Pulse compression

4.1 Self-chirping in nonlinear media

Despite the usual attempts researchers take in trying to avoid the undesirable effects of the nonlinear response on the high-power pulses, it might be possible to employ these phenomena to further compress ultrashort pulses. When an optical pulse propagates through a media, the refractive index of the latter changes according to Eq. (7), following the intensity of the optical field (the Kerr effect). Phase velocity, $v_p=c/n$, varies accordingly. The field frequency of the pulse, whose phase velocity continuously changes, shifts proportionally to its derivative dv_p/dt, so generating pulse chirping. Fig. 10 illustrates this process.

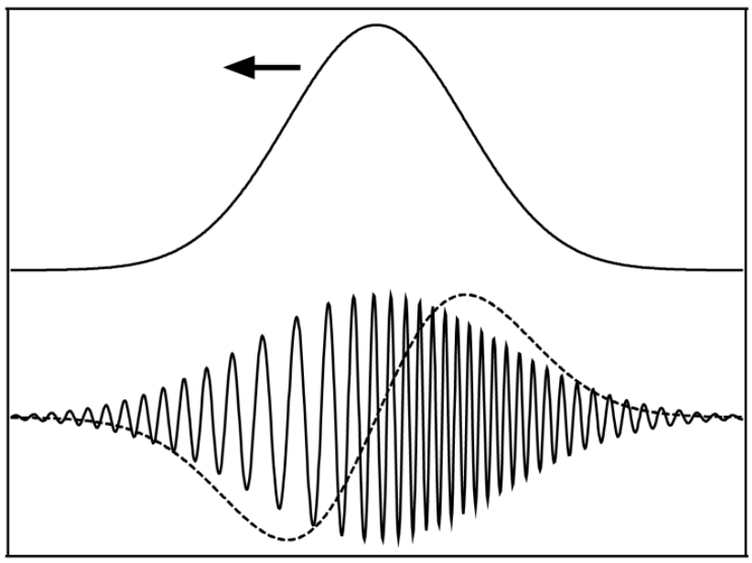

Fig. 10. Self-chirping of a pulse propagating through a nonlinear media. Top: Pulse intensity profile (leading edge is on the left); bottom dashed: Phase velocity derivative; bottom solid: Wave-packet of the chirped pulse.

It is important to realize the difference between the chirping, as in the CPA, and chirping, as in self-chirping. In the first case, the pulse's spectrum is unchanged whereas its duration increases; in the second, the spectrum broadens while pulse duration does not change. A dispersive compressor similar to that utilized in the CPA can be arranged to shrink the self-chirped pulse well below its original duration.

4.2 Self-chirping in plasma

Self-chirping in plasma essentially is a variation of the self-chirping in nonlinear media. The distinctive feature of this case is that the variation in refractive index is caused by laser-

induced gas-ionization rather than the Kerr effect. Refractive index of the ionized gas is determined by the linear refractive index of the media, n_0, and the plasma density, N_e:

$$n = n_0 \left(1 - \frac{N_e}{N_c}\right)^{1/2}, \tag{9}$$

where N_c is the critical density (Eq. (1)). Unlike the Kerr effect, where refractive index usually *increases* with laser intensity, strong ionization in high-intensity fields *decreases* the refractive index. Therefore, the direction of chirping is reversed: The field frequency of the leading edge of the pulse is higher than that of the trailing one (*blue chirp*), allowing the compression of the chirped pulse via the linear dispersion in an optical material. By sending the pulse through a window of a properly selected thickness, made of a material with negative group velocity dispersion (e.g., NaCl), we can delay the blue-shifted leading edge of the pulse more than the trailing edge, thus shrinking the pulse.

Inert gases (e.g., xenon) are considered promising candidates for the role of nonlinear media for CO_2 laser pulse self-chirping (Gordienko et al., 2009). A complication arises because the field intensity is not constant across the beam; thus, self-chirping that is pronounced in the center of the beam becomes negligible at its edges. The beam can be homogenized using a hollow waveguide (Nisoli et al., 1997, Voronin et al., 2010), or a filamentation regime (Couairon et al., 2006, Gordienko et al., 2009). Fig. 11 shows the results of simulations of an 1.2-ps pulse compression via self-chirping in xenon in filamentation regime followed by a NaCl compressor.

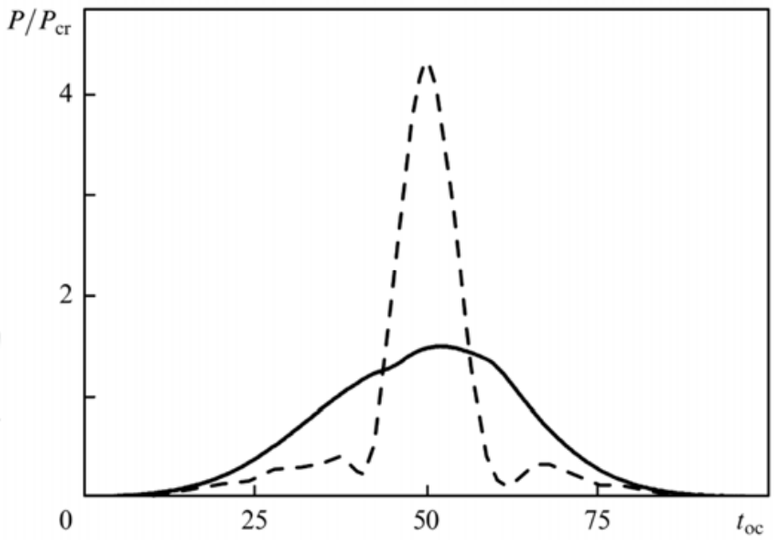

Fig. 11. Simulated 1.2-ps (FWHM) pulse before (solid) and after (dashed) compression via self-chirping in xenon plasma and dispersive compression in NaCl (Gordienko et al., 2009). Time is measured in optical cycles (1 o.c.≈35 fs); P is power and P_{cr} is critical self-focusing power in xenon: $P_{cr} \approx \lambda^2/4\pi n_0 n_2$. Reprinted by permission of Turpion Ltd.

Corcum observed unintentional pulse shortening due to plasma chirping in a picosecond CO_2 amplifier (Corcum, 1985). The suggested explanation capitalized on the pulse's self-

chirping in the partially ionized active media, and compression in the material of the cavity windows. Controlled shortening was realized using an external gas cell by Tochitsky et al. (Tochitsky et al., 2001).

5. Pulse diagnostics

Measuring the temporal structure of ultrashort 10-μm pulses is not fundamentally different from measuring visible or near-IR pulses. However, due to low demand, there are very few commercial diagnostic instruments (e.g., Frequency Resolved Optical Gating, FROG) suitable for direct use in the mid-IR region. Several techniques used for diagnosing CO_2 laser pulses are schematically represented in Fig. 12.

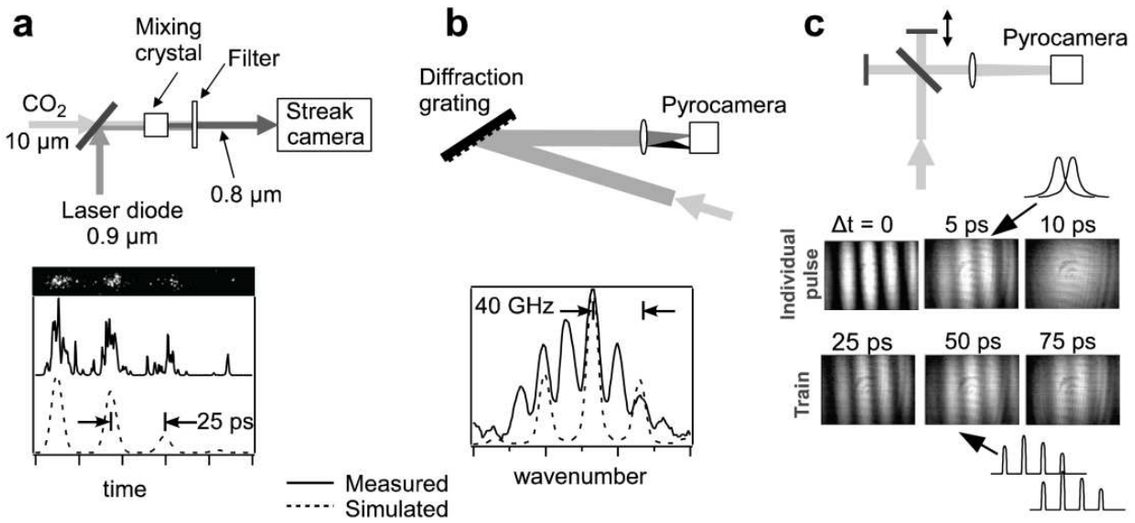

Fig. 12. Apparatuses for ultrashort mid-IR pulse diagnostics. (a) Streak camera; (b) Spectrometer (additional peaks in the measured spectrum are attributed to a sequence band not included in the simulations); and, (c) Autocorrelator.

A *streak camera* is a convenient tool for monitoring the pulse structure, providing a resolution of 1-2 ps. Because photocathodes used in streak cameras are insensitive to the mid-IR wavelengths, a frequency conversion technique must be used to shift the pulse wavelength to the visible- or near-IR- diapason. For this purpose, either a difference-frequency mixing in a nonlinear crystal (Fig. 12a), or a Kerr-cell-based optical switch where the CO_2 laser's pulse controls a visible or mid-IR beam is suitable. The resolution of the streak camera is sufficient for measuring pulse splitting due to modulation on the rotational gain spectrum. However, the accuracy of measuring the duration of individual pulses is limited by 1-2 ps.

A *spectrometer* can be used for indirect measurement of the pulse's duration. In the absence of chirping, the total bandwidth of the spectrum is inversely proportional to the duration of the individual pulses (Eq. (2)). If the beam's quality is good enough, a simple grating spectrometer can be arranged similar to that shown in Fig. 12b.

An *autocorrelator* technique must be established to attain the most reliable results. For instance, it can be used to periodically validate the measurements from the streak camera and the spectrometer. An autocorrelator splits the measured beam into two, and recombines it on an active element where the pulses interact, providing a measurable signal that is a function of the temporal overlap. By recording the interaction signal as a function of the time-delay between pulses, we obtain information about the temporal profile of the pulse. Usually, a nonlinear crystal is used as the active element, generating a harmonic frequency when the two pulses overlap in time. In a simpler design, the pulses' temporal overlap is evaluated by measuring the modulation of the interference pattern resulting from the interaction of the two beams. In the autocorrelator design shown in the Fig. 12c an intentionally induced slight misalignment of the interferometer's arms generates an interference pattern on the pyroelectric camera's sensor. The interference contrast serves as a measure of the temporal overlap between the pulses; the maximum modulation corresponds to zero delay, whereas the complete separation of the pulses in time entails the disappearance of interference. With this technique, we can study both the duration of individual pulses and the train's structure, which results in the periodic appearance of the interference pattern with gradually reduced modulation at delays that are multiples of the pulse-splitting period.

6. Existing terawatt CO_2 lasers

Two systems worldwide now can generate terawatt peak-power, 10-μm pulses: One at the Accelerator Test Facility of the Brookhaven National Laboratory (BNL) (Polyanskiy et al., 2011); and, the other at the Neptune Laboratory of the University of California, Loss Angeles (UCLA) (Haberberger et al., 2010). These systems are described briefly below.

6.1 1-TW system at BNL's Accelerator Test Facility (BNL-ATF)

The CO_2 laser system depicted in the Fig. 13 consists of a picosecond pulse-generator that produces a linear-polarized 0.1-μJ, 5-ps pulse, along with two high-pressure amplifiers that ultimately boost the laser pulses' energy to the ~5 J level.

In this system, a 5-ps pulse is sliced by the sequence of optical switches from the 200-ns, 20-mJ output of a hybrid TEA CO_2 laser tuned to the 10R(14) line (10.3 μm). First, a 10-ns pulse is cut off the initial pulse with a Pockels cell, and intensified in a 3-bar UV-pre-ionized electric-discharge pre-amplifier. Then, a semiconductor optical switch, which is controlled by a 14-ps YAG laser, slices off a ~200 ps part of the pulse. Finally, the 200-ps pulse is sent through a CS_2 Kerr cell controlled by a co-propagating, 5-ps, frequency-doubled YAG laser-pulse. A polarization filter placed after the Kerr cell selects a 0.1-μJ, 5-ps seed pulse that then is raised to 10 mJ in multiple round-trip passes through a regenerative amplifier filled with a gas mixture featuring *isotopically enriched* carbon dioxide to prevent pulse splitting upon amplification. The amplifier is energized with UV-pre-ionized transverse electric discharge. Further amplification to 5 J is attained in 6 passes through a large-aperture (8x10 cm^2), x-ray pre-ionized final amplifier. Field broadening prevents pulse splitting in the final amplifier despite using regular CO_2 gas therein. The output is a single 5-ps pulse implying ~1 TW peak power. Table 2 summarizes the technical details of these two amplification stages.

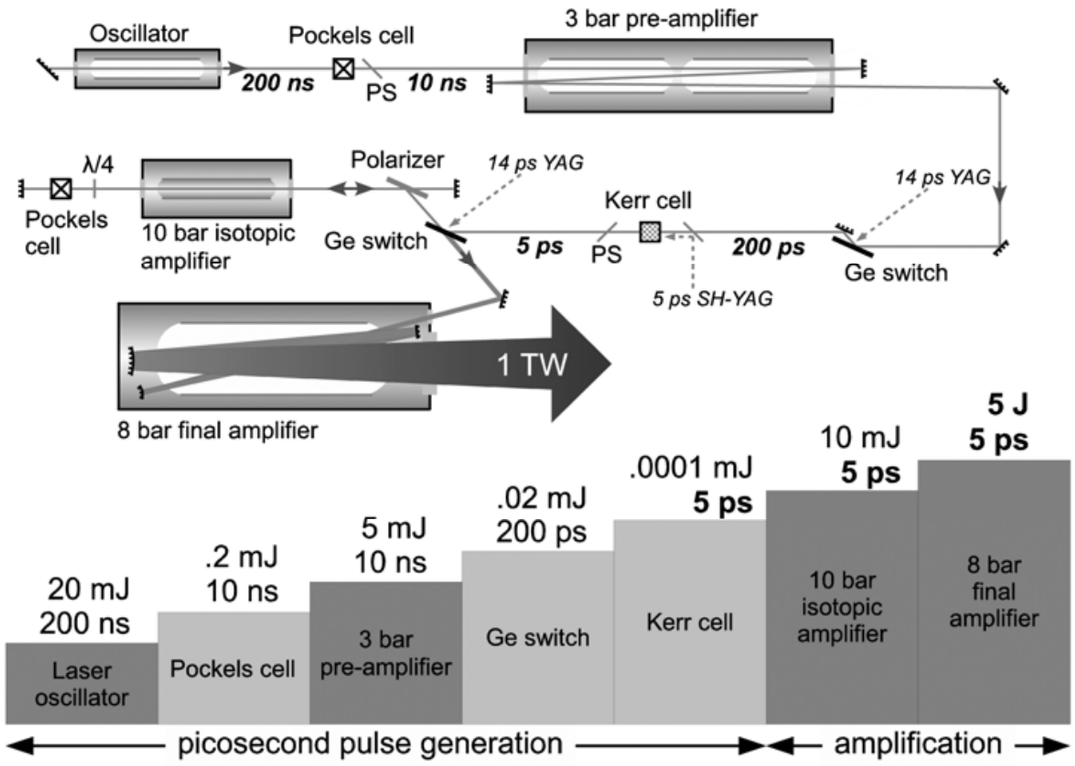

Fig. 13. Layout and pulse dynamics in the BNL-ATF CO_2 laser system; PS: Polarizing splitter.

	Regenerative amplifier	**Final amplifier**
Working pressure	10 bar	8 bar
Gas mixture: $[CO_2]:[N_2]:[He]$	1:1:18 (isotopic CO_2)	2:1:28
Active volume	1×1×80 cm^3	8×10×100 cm^3
Small-signal gain	1-2 %/cm	1.5-2 %/cm
Number of passes	8-12 round-trips	6 passes
Net amplification	10^5	10^3

Table 2. Parameters of BNL-ATF laser amplifiers.

6.2 15-TW system at UCLA's Neptune Laboratory

Fig. 14 is a scheme of the CO_2 laser system of the UCLA's Neptune Laboratory operating at 10.6 μm wavelength (10P branch). The 3-ps injection pulse is produced by slicing a portion of the output of a hybrid TEA CO_2 laser (comprising a low-pressure smoothing tube to suppress energy modulation caused by self-mode-locking). The slicing is realized as a single-step process, using a CS_2-filled Kerr cell controlled by a 3-ps pulse of a solid-state laser. The nanojoule injection pulse first is amplified in an 8-bar regenerative amplifier,

reaching milijoules energy and splitting into a train of ~7 sub-pulses separated by 18-ps intervals. The final 2.5-bar amplifier boosts the pulse energy up to 100 J, and simultaneously mostly suppresses splitting via the field-broadening effect. The output pulse consists of 2-3 sub-pulses with ~45% energy in the first of them, implying ~15 TW peak power.

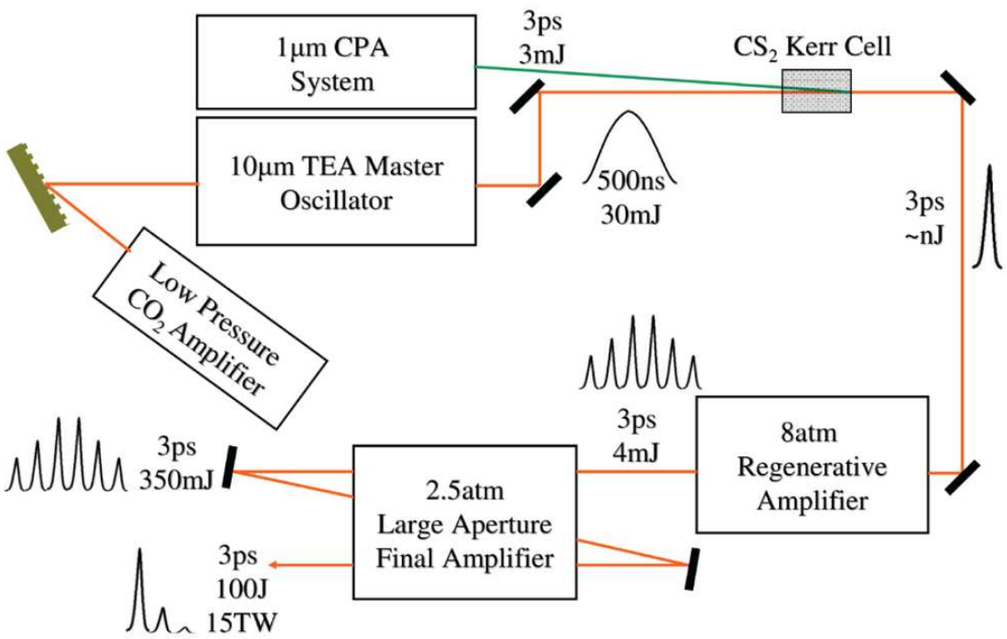

Fig. 14. Layout and pulse dynamics of the UCLA's Neptune Laboratory laser system (Haberberger et al., 2010). Reproduced with permission.

Table 3 summarizes the parameters of this system's amplifiers.

	Regenerative amplifier	**Final amplifier**
Working pressure	8 bar	2.5 bar
Gas mixture: $[CO_2]$:$[N_2]$:[He]	1:1:14	4:1:0
Active volume	1×1×60 cm^3	20×35×250 cm^3
Small-signal gain	-	2.6 %/cm
Number of passes	-	3 passes
Net amplification	10^7	10^5

Table 3. Parameters of UCLA's Neptune Laboratory laser amplifiers.

7. Conclusion

We overviewed the underlying physics and technical approaches to generating and amplifying ultrashort 10-μm pulses. Modern CO_2 laser systems can generate pulses as brief as few picoseconds and as powerful as several terawatt. Potential applications, among

which are the high-energy physics experiments and the proton acceleration for cancer therapy, call for even higher peak power.

Achievements in solid-state laser technology can help the further development of ultrashort-pulse, high-peak-power CO_2 laser systems. Modern solid-state lasers can be directly used in mid-IR systems, e.g., for controlling optical switches, pumping CO_2 laser transition, or generating the ultrashort 10-μm seed pulses via nonlinear frequency conversion and parametric amplification. Apart from that, the advanced techniques initially developed for solid-state lasers (e.g. chirped pulse amplification) can be adopted in CO_2 laser systems.

8. Acknowledgements

This work is supported by the US DOE contract DE-AC02-98CH10886 and by the BNL Laboratory Directed R&D (LDRD) grant #07-004. The authors are thankful to Sergei Tochitsky from UCLA's Neptune Laboratory for providing information on the Neptune's CO_2 laser.

9. References

Abrams, R. L. & Wood, O. R. (1971). Characteristics of a mode-locked TEA CO_2 laser. *Appl. Phys. Lett.,* Vol.19, No.12, (December 1971), pp. 518-520, ISSN 0003-6951

Alcock, A. J. & Corkum, P. B. (1979). Ultra-fast switching of infrared radiation by laser-produced carriers in semiconductors. *Can. J. Phys.,* Vol.57, No.9, (September 1979), pp. 1280-1290, ISSN 0008-4204

Armstrong, J. A., Bloembergen, N., Ducuing, J. & Pershan, P. S. (1962). Interactions between light waves in a nonlinear dielectric. *Phys. Rev.*, Vol.127,No.6, (September 1962), pp. 1918-1939, ISSN 1943-2879

Autler, S. H. & Townes, C. H. (1955). Stark effect in rapidly varying fields. *Phys. Rev.*, Vol.100,No.2, (October 1955), pp. 703-722, ISSN 1943-2879

Brimacombe, R. K. & Reid, J. (1983). Accurate measurements of pressure-broadened linewidths in a transversely excited CO_2 discharge. *IEEE J. Quantum Electron.,* Vol.19, No.11, (November 1983), pp. 1668-1673, ISSN 0018-9197

Bristow, A. D., Rotenberg, N., & van Driel, H. M. (2007). Two-photon absorption and Kerr coefficients of silicon for 850–2200 nm. *Appl. Phys. Lett.*, Vol.90, No.19 (May 2007), p. 191104, ISSN 0003-6951

Corkum, P. B. & Krausz, F. (2007). Attosecond science. *Nature Physics.,* Vol.3, No.6, (June 2007), pp. 381-387, ISSN 1745-2473

Corkum, P. B. (1983). High-power, subpicosecond 10-μm pulse generation. *Opt. Lett.*, Vol.8, No.10, (October 1983), pp. 514-516, ISSN 0146-9592

Corkum, P. B. (1985). Amplification of picosecond 10 μm pulses in multiatmosphere CO_2 lasers. *IEEE J. Quantum Electron.,* Vol.21, No.3, (March 1985), pp. 216-232, ISSN 0018-9197

Couairon, A., Biegert, J., Hauri, C. P., Kornelis, W., Helbing, F. W., Keller, U. & Mysyrowicz, A., F. (2006). Self-compression of ultra-short laser pulses down to one optical cycle by filamentation. *J. Modern Opt.,* Vol.53, No.1-2, (January 2006), pp. 75-85, ISSN 0950–0340

Du, D., Liu, X., Korn, G., Squier, J., & Mourou, G. (1994). Laser-induced breakdown by impact ionization in SiO_2 with pulse widths from 7 ns to 150 fs. *Appl. Phys.Lett.*, Vol.64, No.26 (June 1994), pp. 3071-3073, ISSN 0003-6951

Esirkepov, T., Borghesi, M., Bulanov, S. V., Mourou, G. & Tajima, T. (2004). Highly efficient relativistic-ion generation in the laser-piston regime. *Phys. Rev. Lett.,* Vol.92, No.17 (April 2004), p. 175003, ISSN 0031-9007

Filip, C. V., Narang R., Tochitsky, S. Ya., Clayton, C. E. &. Joshi, C. (2002). Optical Kerr switching technique for the production of a picosecond, multiwavelength CO_2 laser pulse. *Appl. Opt.*, Vol.41, No.18, (June 2002), pp. 3743-3747, ISSN 0003-6935

Giordmaine, J. A. & Miller, R. C. (1965). Tunable coherent parametric oscillation in $LiNbO_3$ at optical frequencies. *Phys. Rev. Lett.,* Vol.14, No.24 (June 1965), p. 973-976, ISSN 0031-9007

Gordienko, V. M., & Platonenko, V. T. (2010). Regenerative amplification of picosecond 10-μm pulses in a high-pressure optically pumped CO_2 laser. *Quant. Electron.*, Vol.40, No.12, (December 2009), pp. 1118-1122, ISSN 1063-7818

Gordienko, V. M., Platonenko, V. T. & Sterzhantov, A. F. (2009). Self-action of a high-power 10-μm laser radiation in gases: control of the pulse duration and generation of hot electrons. *Quant. Electron.*, Vol.39, No.7, (July 2009), pp. 663-668, ISSN 1063-7818

Haberberger, D., Tochitsky, S. & Joshi, C. (2010). Fifteen terawatt picosecond CO_2 laser system. *Opt. Express*, Vol.18, No.17, (August 2010), pp. 17865-17875, ISSN 1094-4087

Houfman, H. & Meyer, J. (1987). Ultrashort CO_2 laser pulse generation by square-wave mode locking and cavity dumping. *Opt. Lett.,* Vol.12, No.2, (February 1987), pp. 87-89, ISSN 0146-9592

Jia, T. Q., Chen, H. X., Huang, M., Zhao, F. L., Li, X. X., Xu, S. Z., Sun, H. Y., Feng, D. H., Li, C. B., Wang, X. F., Li, R. X., Xu, Z. Z., He, X. K. & Kuroda, H. (2006). Ultraviolet-infrared femtosecond laser-induced damage in fused silica and CaF_2 crystals. *Phys. Rev. B*, Vol.73, No.5 (February, 2006) p.054105, ISSN 0163-1829

Korzhimanov, A. V., Gonoskov, A. A., Khazanov, E. A. & Sergeev, A. M. (2011). Horizons of petawatt laser technology. *Physics - Uspekhi,* Vol.54, No.1, (January 2011), pp. 9-28, ISSN 1063-7869

Kovalev, V. I. (1996). Mechanism of self-mode-locking in the active medium of CO_2 lasers. *Quant. Electron.,* Vol.26, No.2, (February 1996), pp. 131-132, ISSN 1063-7818

Nisoli, M., Stagira, S., De Silvestri, S., Svelto, O., Sartania, S., Cheng, Z., Lenzner, M., Spielmann, C. & Krausz, F. (1997). A novel high-energy pulse compression system: generation of multigigawatt sub-5-fs pulses. *Appl. Phys. B,* Vol.65, No.2, (August 1997), pp. 189-196, ISSN 0946-2171

Norreys, P. (2011). Particle acceleration: Pushing protons with photons. *Nature Photonics,* Vol.5, No.3, (March 2011), pp. 134-135, ISSN 1749-4885

Okorogu, A. O., Mirov, S. B., Lee, W., Crouthamel, D. I., Jenkins, N., Dergachev, A. Yu., Vodopyanov, K. L. & Badikov, V. V. (1998). Tunable middle infrared downconversion in GaSe and $AgGaS_2$. Opt. Commun., Vol.155, No.4-6, (October 1998), pp. 307-312, ISSN 0030-4018

Palmer, C. A. J., Dover, N. P., Pogorelsky, I., Babzien, M., Dudnikova, G. I., Ispiriyan, M., Polyanskiy, M. N., Schreiber, J., Shkolnikov, P., Yakimenko, V. & Najmudin, Z.

(2011). Monoenergetic proton beams accelerated by a radiation pressure driven shock. *Phys. Rev. Lett.,* Vol.106, No.1 (January 2011), p. 014801, ISSN 0031-9007

Paschotta, R. (2008). *Field Guide to Laser Pulse Generation,* SPIE Press, ISBN 978-0-8194-7248-9, Bellingham, Washington, USA

Paschotta, R.. B-Integral. *Encyclopedia of laser physics and technology*. Available from: http://www.rp-photonics.com/b_integral.html. Accessed October 6, 2011

Perry, M., Shore, B., Boyd, R. & Britten, J. (1995). Multilayer dielectric gratings: Increasing the power of light. LLNL Sci. Technol. Rev., (September 1995), pp. 24-33

Polyanskiy, M. N., Pogorelsky, I. V. & Yakimenko, V. (2011). Picosecond pulse amplification in isotopic CO_2 active medium. *Opt. Express*, Vol.19, No.8, (April 2011), pp. 7717-7725, ISSN 1094-4087

RefractiveIndex.INFO. *Refractive index database.* Available from http://refractiveindex.info. Accessed September 30, 2011

Reid, J. & Siemsen, K. (1976). New CO_2 laser bands in the 9–11-μm wavelength region. *Appl. Phys. Lett.*, Vol.29, No.4 (August 1976), pp. 250-251, ISSN 0003-6951

Rolland, C. & Corkum, P. B. (1986). Generation of 130-fsec midinfrared pulses. *J. Opt. Soc. Am. B,* Vol.3, No.12, (December 1986), pp. 1625-1629, ISSN 0740-3224

Rothman, L. S., Gordon, I. E., Barbe, A. et al. (2009) The HITRAN 2008 molecular spectroscopic database. *J. Quant. Spectr. Rad. Transfer,* Vol.110, No.9-10 (June-July 2009), pp. 533-572, ISSN: 0022-4073

Sheik-Bahae, M., Hutchings, D. C., Hagan, D. J. & Van Stryland, E. W. (1991). Dispersion of bound electron nonlinear refraction in solids. *IEEE J. Quantum Electron.,* Vol.27, No.6, (June 1991), pp. 1296-1309, ISSN 0018-9197

Siegman, A. E. & Kuizenga, D. J. (1969). Simple analytical expressions for AM and FM mode-locked pulses in homogeneous lasers. *Appl. Phys. Lett.,* Vol.14, No.6, (March 1969), pp. 518-520, ISSN 0003-6951

Stuart, B. C., Feit, M. D., Rubenchik, A. M., Shore, B. W., and Perry, M. D. (1996). Nanosecond-to-femtosecond laser-induced breakdown in dielectrics. *Phys. Rev. B*, Vol.53, No.4, (January 1996), pp. 1749-1761, ISSN 0163-1829

Tien, A.-C., Backus, S., Kapteyn, H., Murnane M., & Mourou G. (1999). Short-pulse laser damage in transparent materials as a function of pulse duration. *Phys. Rev. Lett.*, Vol.82, No.19 (May 1999), pp. 3883-3886, ISSN 0031-9007

Tochitsky, S. Ya., Filip, C., Narang, R., Clayton, C. E., Marsh, K. A. & Joshi, C. (2001). Efficient shortening of self-chirped picosecond pulses in a high-power CO_2 amplifier. *Opt. Lett.,* Vol.26, No.11, (June 2001), pp. 813-815, ISSN 0146-9592

Voronin, A. A., Gordienko, V. M., Platonenko, V. T., Panchenko, V. Ya. & Zheltikov, A. M. (2010). Ionization-assisted guided-wave pulse compression to extreme peak powers and single-cycle pulse widths in the mid-infrared. *Opt. Lett.,* Vol.35, No.21, (November 2010), pp. 3640-3642, ISSN 0146-9592

Witteman, W. J. (1987). *The CO_2 laser*. Springer-Verlag, ISBN 0-387-17657-8, Berlin Heidelberg New York London Paris Tokyo

Wood, O. R., Abrams R. L. & Bridges, T. J. (1970). Mode locking of a transversively excited atmospheric pressure CO_2 Laseer. *Appl. Phys. Lett.,* Vol.17, No.9, (November 1970), pp. 376-378, ISSN 0003-6951

Yablonovich, E. (1973). Spectral broadening in the light transmitted through a rapidly growing plasma. *Phys. Rev. Lett.,* Vol.31, No.14, (October 1973), pp. 877–879, ISSN 0031-9007

Yablonovich, E. (1974a). Short CO_2 laser pulse generation by optical free induction decay. *Appl. Phys. Lett.,* Vol.25, No.10, (November 1974), pp. 580-582, ISSN 0003-6951

Yablonovich, E. (1974b). Self-phase modulation and short-pulse generation from laser-breakdown plasmas. *Phys. Rev. A,* Vol.10, No.5, (November 1974), pp. 1888-1895, ISSN 1050-2947

Yakimenlo, V. & Pogorelsky, I. (2006). Polarized γ source based on Compton backscattering in a laser cavity. *Phys. Rev. ST Accel. Beams,* Vol.9, No.9, (September 2006), p. 091001, ISSN 1098-4402

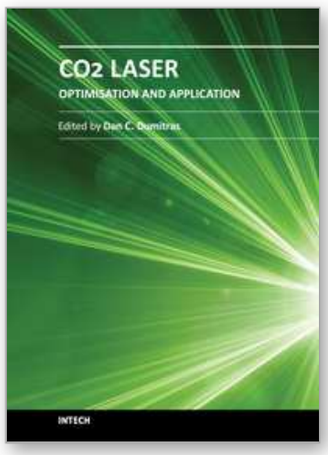

CO2 Laser - Optimisation and Application
Edited by Dr. Dan C. Dumitras

ISBN 978-953-51-0351-6
Hard cover, 436 pages
Publisher InTech
Published online 21, March, 2012
Published in print edition March, 2012

The present book includes several contributions aiming a deeper understanding of the basic processes in the operation of CO2 lasers (lasing on non-traditional bands, frequency stabilization, photoacoustic spectroscopy) and achievement of new systems (CO2 lasers generating ultrashort pulses or high average power, lasers based on diffusion cooled V-fold geometry, transmission of IR radiation through hollow core microstructured fibers). The second part of the book is dedicated to applications in material processing (heat treatment, welding, synthesis of new materials, micro fluidics) and in medicine (clinical applications, dentistry, non-ablative therapy, acceleration of protons for cancer treatment).

InTech Europe
University Campus STeP Ri
Slavka Krautzeka 83/A
51000 Rijeka, Croatia
Phone: +385 (51) 770 447
Fax: +385 (51) 686 166
www.intechopen.com

InTech China
Unit 405, Office Block, Hotel Equatorial Shanghai
No.65, Yan An Road (West), Shanghai, 200040, China
中国上海市延安西路65号上海国际贵都大饭店办公楼405单元
Phone: +86-21-62489820
Fax: +86-21-62489821

IntechOpen